Investigating the role of Arp2/3 and formins in neuronal growth cones

B.S – M.S Thesis

Beeraka Sai Prashanth Kumar

20091032

Under guidance of

Dr. Aurnab Ghose

Biology department, IISER Pune

Certificate

This is to certify that this dissertation entitled “Investigating the role of Arp2/3 and formins in neuronal growth cones” towards the partial fulfillment of the BS-MS dual degree program at the Indian Institute of Science Education and Research, Pune represents original research carried out by Beeraka Sai Prashanth Kumar at IISER Pune under the supervision of Dr. Aurnab Ghose, Assistant Professor, Biology Division, IISER Pune during the academic year 2013-2014.

Dr. Aurnab Ghose
Assistant Professor
Biology Division, IISER Pune

Declaration

I hereby declare that the matter embodied in the report “Investigating the role of Arp2/3 and formins in neuronal growth cones” are the results of the investigations carried out by me at the Department of Biology, IISER Pune, under the supervision of Dr. Aurnab Ghose and the same has not been submitted elsewhere for any other degree.

Beeraka Sai Prashanth Kumar
B.S – M.S Dual Degree Student
IISER Pune

Abstract

Actin is involved in various aspects of cellular motility, including growth cone-dependent translocation and guidance of axons. During cellular motility actin is pivotal in generating protrusive structures, like filopodia and lamellipodia, and development of substrate adhesions and traction forces. Actin nucleation is a major regulator of actin dynamics and multiple actin nucleators, including the Arp2/3 complex and formins are expressed in the developing nervous system. In this study, specific pharmacological inhibition of the Arp2/3 complex and formin based nucleation is employed to compare and contrast the functional significance of these nucleators in neuronal growth cones. We find Arp2/3 regulates the spreading of the growth cones but not filopodia or translocation rates. Further, Arp2/3 is necessary for cue-dependant directional turning of growth cones. formins, on the other hand, regulate filopodia and are central to translocation as inhibition of formin activity reduces growth rates possibly by modulating the underlying adhesive structures.

Additionally, in order to aid detailed microscopic analysis of actin structures in growth cones and the regulation of stress fiber formation and maintenance by actin nucleators, I have developed photo-activatable constructs and FRAP analysis of stress fiber dynamics.

List of figures

Acknowledgements

I take this opportunity to thank my mentor Dr. Aurnab Ghose for his valuable, inspiring and encouraging guidance and for providing me with scientific freedom that enabled me to work enthusiastically and molded my scientific development.
I would like to thank Dr. Richa Rikhy, for her valuable inputs and all my lab members Abhishek, Ketakee, Tanushree, Sampada, Akash, and Tarun for assisting, teaching, and encouraging me all through the project and for maintaining a fun atmosphere in the lab.
I thank my friends, and family for showing faith and providing confidence during my entire IISER life.

Table of Contents

CHAPTER 1

Introduction:

The cytoskeleton

Physiological functions of the vast repertoire of cell types often dictate their morphologies. The underlying cytoskeleton, comprising of a dynamic network of interconnected actin filaments and microtubules, provides an extensive variation in the cell shape (Chesarone et al., 2010). The cytoskeleton also plays a major role in regulating cell polarization, cell division, intracellular cargo trafficking, anchorage and cell mobility (Ruiz-Cañada and Budnik, 2006).Bio chemical interactions modulate the dynamics of these polymers. The assembly and disassembly of these polymeric structures ultimately translates to functional specificity.

Among the three major components of the cytoskeleton, actin is one of the most abundant. Actin homologues have been shown to be present in prokaryotes and seem to be important for polarity and morphogenesis. Actin monomer (globular; G-actin), is 43 kiloDalton (kDa) protein comprising of about 375 amino acids, is highly conserved in eukaryotes with higher eukaryotes having multiple isoforms of actin (α, β and γ). Actin binds adenosine tri-phosphate (ATP) which is hydrolyzed to adenosine di-phosphate (ADP) leading to the formation of filamentous (F) actin. These filaments typically have a diameter of about 7 – 10 nm with varying lengths depending upon other factors. Actin monomers are capable of self assembly and to keep this under control the cell engages a vast repertoire of actin associated proteins that maintain a pool of G-actin, initiate polymerization and modulate assembly and turnover of the actin filaments and also crosslink them with other components of the cell (Pollard and Cooper, 2009; Riedl, 2010). An important group of actin binding proteins (ABPs) are ones that orchestrate *de novo* polymerization. The mechanism of polymerization can be divided in to two phases – nucleation and elongation. Nucleation can result from actin monomer, branching from existing filaments or by providing new ends by severing existing filaments. Once

nucleated, actin monomers are added to the barbed ends (fast growing ends). Elongation also occurs at a slower rate at the pointed end, but is constraint by many proteins that bind the pointed end. On the contrary, actin monomers dissociate from the pointed leading to a steady state turnover known as actin filament treadmilling (Dominguez, 2009).

Neurons as a model to study cytoskeletal dynamics

The cytoskeletal dynamics are critical for neuronal cells. These cells send out projections which can contact other cells away from them, sometimes even meters away. This can be attributed to its cytoskeleton which provides mechanical support as well as driving force for the neuronal projection. Among the many projections that protrude out of the cell body, one gets stochastically chosen to be the axon. At the tip of each growing axon is a growth cone, first described by Ramon y Cajal in 1890. Cajal recognized that growth cones were conical structures with finger-like projections that navigate during axon pathfinding, ultimately leading to their synaptic targets (Henley and Poo, 2011)(Gomez and Letourneau, 2013). These projections are known to actively extend and retract during navigation. This behavior arises due to the dynamic assembly and turnover of the underlying cytoskeleton. Actin rich leading edge, Peripheral (P) domain, of the growth cone comprises the finger like, filopodial projections, along with broad lamellipodia. Bundled actin filaments give rise to filopodial structure while the branched actin filaments support the lamellipodia. Behind the P domain, the central (C) domain comprises the more stable bundled microtubules whose dynamics are controlled partly by the actin organization. Between the two sits the transition (T) zone (Lowery and Van Vactor, 2009).The membrane encompassing these structures bears receptors which detect ligands or guidance cues. These external cues can activate or inhibit membrane receptors which regulate cytoskeletal dynamics and hence, guide the growth cone machinery. These cues can act as attractants or repellents in the form of substrate bound or diffusible molecules which trigger a cascade of downstream signaling events, thereby determining the direction of growth cone extension(Jin et al., 2005; Ming et al., 1997). Ultimately these signals are transduced to the cytoskeletal

dynamism. Thus, the cytoskeletal architecture is continually modified to promote protrusion, adhesion and traction to steer the growth cone. Many proteins that regulate cytoskeletal dynamics in non-neuronal cells, have come to light, but much needs to be learned about signaling components in neuronal cells. The dynamics of these cytoskeletal components determine growth cone shape and movement on its journey during development.

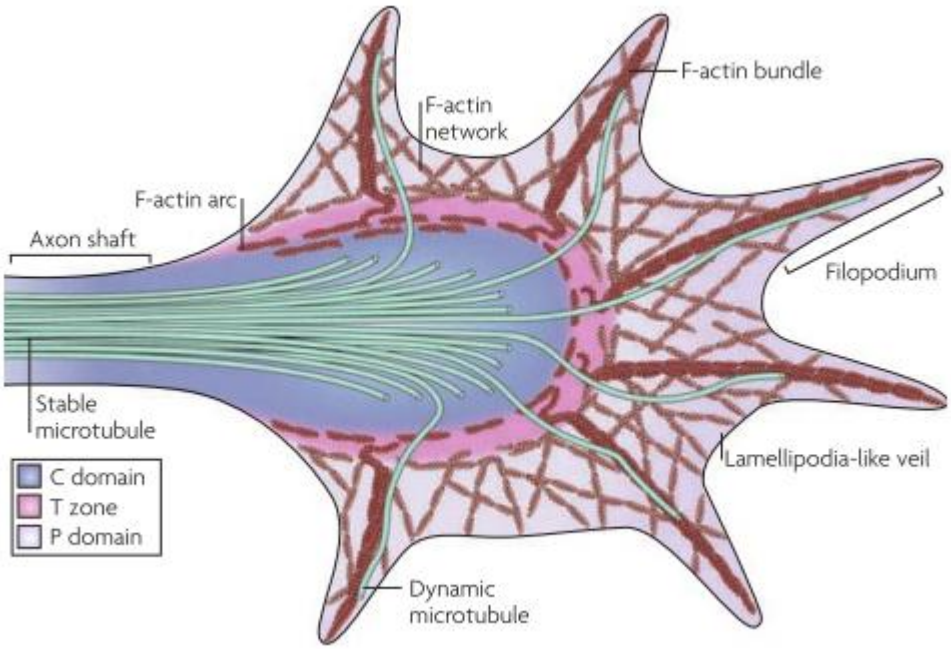

Figure 1: Schematic structure of the growth cone. The leading edge consists filopodia, and lamellipodia. The shape of the growth cone is determined by the underlying cytoskeletal elements. The growth cone can be separated into three domains based on cytoskeletal distribution. The filopodia contains long, bundled actin filaments (F-actin bundles), while the lamellipodia consists of mesh-like branched F-actin networks. 'Pioneer' microtubules (MTs) occasionally explore this region, usually along F-actin bundles. The central (C) domain encloses stable bundled MTs.. The transition (T) zone lies between the P and C domain. [Adapted from (Lowery and Van Vactor, 2009)]

Actin Nucleators

Cytoplasmic G-actin concentrations, which range from 100 to 500 μM, are usually much higher than the critical concentration of G-actin (0.1 μM), at which actin spontaneously polymerizes to form filaments (Pollard and Borisy, 2003).However, ABPs like profilin and thymosin β4 sequester G-actin and inhibit amok polymerization of actin filaments.

Also, during nucleation, dimers and trimers of G-actin form which are thermodynamically unstable and hence require other nucleation factors for stabilization (Sept and McCammon, 2001). Actin nucleators, which stabilize actin polymerization nuclei, are a recent and rapidly evolving field. Actin nucleator is an ABP which seeds filament formation which in turn grows from its barbed end. Actin nucleators have been characterized into three classes based on their mechanism of nucleation:

- Class I : Actin related protein (Arp)2/3 complex
- Class II : formins (FH2 domain containing proteins)
- Class III : Spire, Cordon bleu (Cobl), Leiomodin (Lmod)

Arp2/3 complex, the first actin nucleator to be identified and is now known to be conserved in nearly all eukaryotes, has seven subunits: Arp2 and Arp3 and the five additional subunits ARPC1-5. Unique to this class of nucleators, Arp2/3 complex binds existing filaments and initiates branched filament at angle of about 70° by remaining at the pointed end of the new filament. By itself, Arp2/3 complex is not a very potent actin nucleator, but interaction with nucleation promoting factors (NPFs) escalates its nucleation activity dramatically (Mullins et al., 1998). Most of these NPFs have a WCA domain, which consists of one or more WASP homology 2 (WH2) domain that bind G-actin and thereby delivers it to the barbed end of Arp2/3 for incorporation. Although, the nucleation of Y- branched arrays of actin filament by Arp2/3 is well characterized, details of the mechanism still remain unclear (Firat-Karalar and Welch, 2011). This could be in part because the ARPC1-5 are poorly understood. In neurons, Arp2/3 has been shown to localize in the Central domain and the leading edge of the P domain of the growth cone of a neuron (Yang et al., 2012; Korobova and Svitkina, 2008; Strasser et al., 2004). Previous studies of knockdown of Arp2/3 by siRNA and functional inhibition in neurons, gave conflicting results. siRNA mediated knockdown suggests that Arp2/3 is required for growth cone motility (Korobova and Svitkina, 2008)while the functionally inhibition shows that it is a hindrance to the motility (Strasser et al., 2004). Functional inhibition was brought about by expressing the CA domain of N-WASP, which binds to Arp2/3 with high affinity but does not activate it. Recently a small molecule inhibitor of Arp2/3 was found out (Sun et al., 2011). Using this drug one can

extract vital information which could resolve the confliction between the earlier studies. Unlike the previous studies, one major difference in that can be incorporated with the use of this drug is that effects of inhibition of Arp2/3 can now be studied after the growth cones have become stable. It would be interesting to determine what the role of Arp2/3 in growth cones with certainty.

formins, a conserved family of actin nucleators which are known to play a role in cytoskeleton assembly and organization, are large, multi domain polypeptides which constitute a diverse protein family and interact with a number of cytoskeletal and signaling partners. They are characterized by C-terminal ~ 400 residue formin homology 2 (FH2) domain adjacent to the proline rich formin homology 1 (FH1) domain. These proteins are grouped into seven subclasses depending on the divergence of the FH2 domain: formin (FMN), Diaphanous (DIA), Disheveled Associated Activators of Morphogenesis(DAAM), formin homology domain proteins (FHOD), Inverted formins (INF), formin related proteins (FRL/FMNL) and Delphilin (Schönichen and Geyer, 2010). Acting as homodimers through the FH2 domain, they serve as binding sites for actin. These, then stabilize actin dimers or trimers and promote elongation by remaining processively associated to the barbed end of the filament preventing capping proteins from binding (Kovar, 2006; Riedl et al., 2008). Actin assembly is carried out through two distinct phases: nucleation and elongation. *In vitro* studies reveal that the core FH2 domain is sufficient to nucleate G-actin (Kovar et al., 2003; Zigmond, 2004). While the FH1 domain binds profilin with low micromolar affinity and hence, is able to regulate delivery of G-actin subunits from actin-profilin complexes to FH2 domain for elongation at barbed ends. Recently, formins have come to be known as potent nucleators of unbranched actin filaments, controlling a variety of morphogenetic and cellular functions. In animals, Formins have been primarily implicated in formation of filopodia, lamellipodia, cytokinetic rings, actin networks and stress fibers (Breitsprecher and Goode, 2013). The roles of formins beyond cytoskeletal assembly still need to be explored.

Our lab have shown from western blots and qPCRs that multiple actin nucleators are expressed in the developing chick spinal cord. Specifically, formin2 was shown to bw

required for axon guidance *in ovo* (unpublished, Abhishek Sahasrabudhe). Specifically, axon guidance in spinal

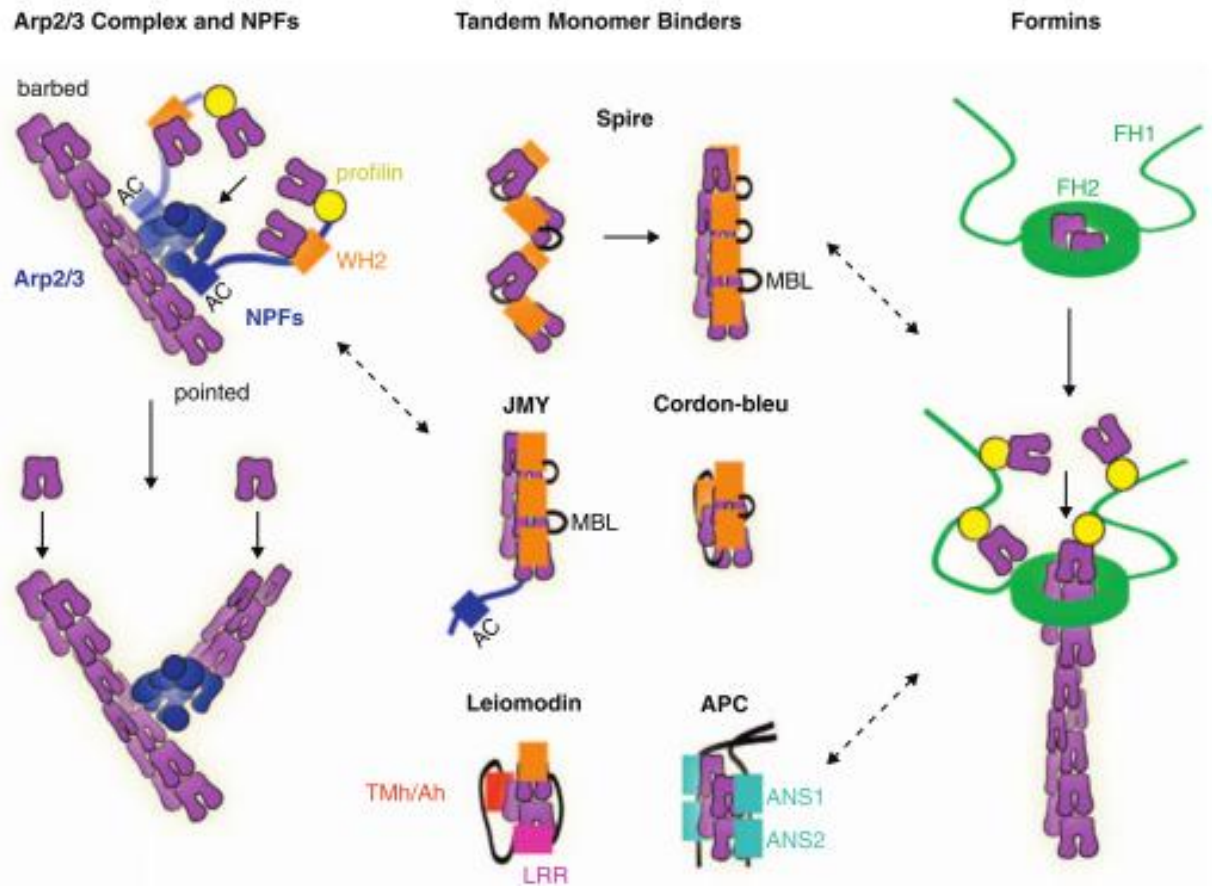

Figure 2: Model for actin nucleation. Arp2/3 complex is activated by binding to the WCA region of NPFs and to the side of actin filaments. In turn, NPFs bind actin monomers via their WH2 domains and profilin-actin monomers to deliver these to the Arp2/3 nucleating complex. Spire and JMY stabilize actin monomers aligned along the long-pitch helix with their WH2 domains. Cordon-bleu, leiomodin and dimeric APC, with their combination of WH2 domains, tropomyosin and actin-binding helices (Tmh/Ah), and actin-nucleating sequences (ANS1-2), stabilize cross-filament interactions along the short- pitch helix of an actin filament. Dotted arrows point to the cross-talk between different actin nucleators. [Adapted from (Firat-Karalar and Welch, 2011)]

interneurons was impaired by knockdown of formin2. This was performed by electroporating morpholinos at stage 14. At this stage the interneurons are still to put out neurites. Allowing them to develop after electroporation would lead to knock down of formin2 and these defects can be visualized at later stages (Embryonic day 4 and 5). Figure 3A shows the projection of a class of interneurons which project contralaterally. The control morpholino transfection, are on the right side of the midline (dotted line) while the trajectories appear on the left. In comparison to this, contra-lateral projections were heavily compromised in spinal columns electroporated with morpholinos for formin2 (Figure 3B). To assess the role actin nucleators in axon guidance, it was preliminary to establish an in vitro assay that could test the effect of the drug inhibitors on during guidance.

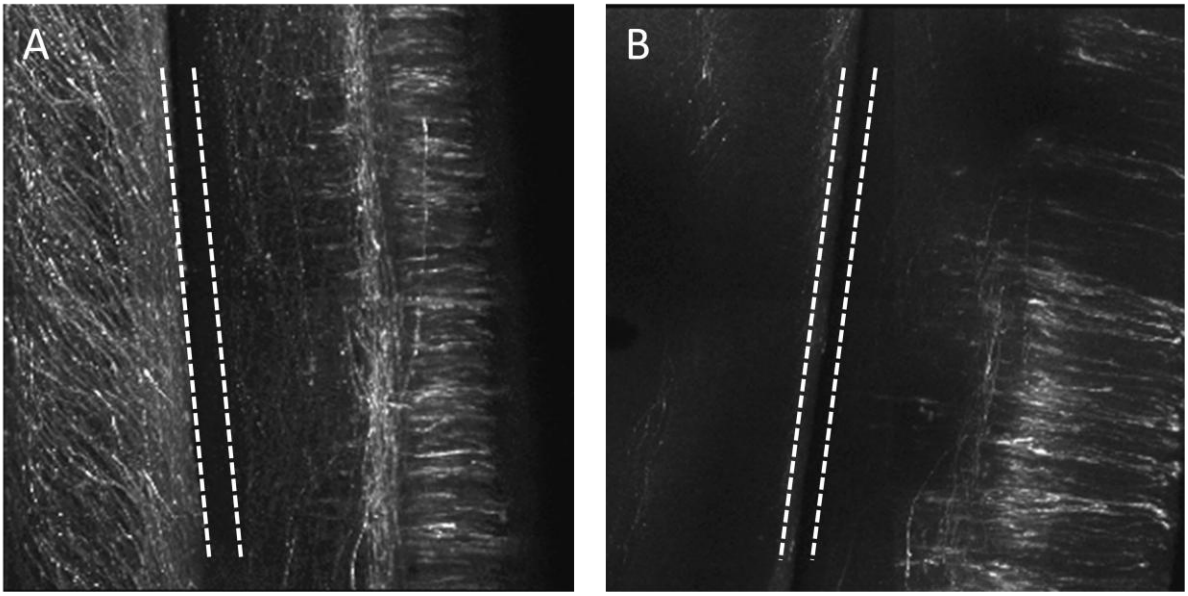

Figure 3: *In ovo* knockdown of formin2. Open book assay with electroporated half on the right side of the midline. (A) Represents the spinal column (E4) electroporated with control morpholinos. Note the trajectories of axon on the left side of the midline. (B) Spinal column (E4) electroporated with morpholinos for formin2. Note the aberrant halting of growth cones before the midline. The dotted line indicates the midline. [Courtesy Abhishek Sahasrabudhe]

A third group actin nucleators has recently come to light that contain a tandem cluster of actin binding motifs. While the WASp-homology 2 (WH2) domain is the most abundant actin-binding motif in this class of nucleators, other potential actin binding elements have been discovered. These WH2 domains may be evolutionarily related to NPFs, but these nucleators haven't yet been implicated in working with Arp2/3. In fact, nucleation by these proteins has been proposed by tethering actin monomers to form single stranded long pitch multimer or short pitch trimers(Campellone and Welch, 2010). Spire, cordon-bleu (Cobl), leiomodin (Lmod) and the more recently identified JMY and adenomatous polyposis coli (APC) belong to this group (Firat-Karalar and Welch, 2011).

To assess the effects of actin nucleators, it is essential to develop an assay that can discern growth cone guidance from a random walk. Inhibiting actin nucleators and studying the response of growth cones through the guidance assay will give us clues to understand the roles of cytokeletal modifiers in neuronal cells.

Visualizing Actin

Fluorescently tagged derivatives of phalloidin, isolated from *Amanita phalloides*, is the most commonly used marker for actin. But this is only restricted to fixed samples and cannot be used in live cell imaging due to toxicity. It irreversibly stabilizes F-actin and prevents depolymerization, thereby leading to cell death. To visualize actin in live cells, researchers have relied on genetically modified actin monomers which are coupled to fluorophores. But theses have their limitations too, as they exhibit reduced functionality. Thus, it can only be used in low concentrations in a background of unlabelled actin. Alternatively, many fusion proteins with actin binding domains have been used to visualize actin. But these proteins are large and to some extent influence actin dynamics.

Recently, a first 17 amino acid sequence, an actin binding protein 140 (Abp140) from the yeast *Saccharomyces cerevisiae*, was shown to comprise the actin binding domain. This sequence, named 'Lifeact', is the shortest actin marker to date and, due to absence of homologous sequence in most eukaryotes, has no known competition from

endogenous actin binding domains. Hence, expressing fluorescently tagged lifeact makes for an undisputed actin marker for live cell imaging. To better understand actin dynamics, it would be reasonable to apply super resolution techniques. By tagging lifeact with photo-activatable/photo-convertible fluorophores, one can resolve actin filaments on a scale of tens of nanometers. Lifeact, possessing a small footprint over actin, is ideal for labeling actin in live cells as it would hinder actin dynamics the least.

Aim of thesis

The role of Arp2/3 in the growth cone is still debatable. With the use of CK666, a small molecule inhibitor of Arp2/3, one might be able to resolve the function of Arp2/3 in maintaining the architecture and dynamics of growth cones. Also, inhibiting formins by using an FH2 domain inhibitor, SMIFH2, one can gain insight into the role of formins in growth cone architecture and dynamics. Results from these experiments would give us a better understanding of actin mediated regulation of growth cone dynamics. Finally, I plan to test whether these actin nucleators play a role in *in vitro* axon guidance. For this purpose, I will be using the chicken (*Gallus gallus domesticus*) embryo Dorsal root ganglion (DRG) as they are robust and easy to culture.

Studies from our lab implicate formins in regulating actin stress fibers. I also attempt to develop tools that will allow super-resolution microscopy of actin structures and ability to assess actin dynamics in stress fiber assembly and maintenance.

CHAPTER 2

Materials and Methods

Materials

L-15 medium, DMEM, B-27 additives, Nerve Growth Factor (NGF), Lipofectamine were obtained from Invitrogen. Poly-l-lysine, laminin were obtained from Sigma.

Cloning pCAG-lifeact-PA GFP / PA mCherry

Primers were obtained from International DNA technologies. The primers were designed keeping in mind the ORFs of both lifeact and PA-GFP / PA-mCherry. The following are the primers used in the for cloning:

pCAG_F: 5`- GCAACGTGCTGGTTATTGTG – 3`

PA-GFP/PAmCherry1_AgeI_F: 5`-GGATCCACCGGTCGCCACCATGGTGAGCAAG GGCGAGGAG–3`

PA-GFP/PAmCherry1_NotI_R: 5`-GAGGAGTGCGGCCGCTTTACTTGTACAGCTCG TCCATG–3`

lifeact_Age1_F: 5 -ATTTAACCGGTATAGCCACCATGGGTGTCGCAGATTTGATC–3`

lifeact_Age1_R: 5`-TTAATACCGGTTCTTCCTTTGAGATGCTTTCGAATTTC–3`

Lifeact (51bp) was amplified by PCR using Pfx polymerase. The primer pair used, lifeact_Age1_F and lifeact_Age1_R, possessed overhangs with Age1 restriction site. PCR product showed a band close to 100bp, on a 0.8% agarose gel, as the overhangs

added 50 more bases to the lifeact. Amplified lifeact was PCR purified, digested with Age1 for 4 hours at 37°C, gel extracted and concentrated by vacuum dessication at 50°C for 30 min.

PA-GFP and PA-mCherry, too, were amplified using the same Pfx polymerase. The primer pairs used for the amplification possessed overhangs for Age1 and Not1. The purified PCR product was double digested with Age1 and Not1 overnight at 37°C.

GFP was excised out of pCAG-GFP (5551bp) plasmid, with ampicillin resistance, by double digestion, overnight, with Age1 and Not1 restriction enzymes (New England Biolabs). Two band, one at 5kb (pCAG) and another at 1kb (GFP), were observed on 2% Agarose gel as expected. The 5 kb band was gel extracted using the QIAGEN Gel extraction kit. The gel extracted product was PCR purified following the protocol of QIAGEN PCR purification kit. PA-GFP and PA-mCherry purified digested products were ligated to the empty digested pCAG vector using TAKARA ligation mix and finally transformed into DH5α competent cells for 1 hour. The transformed cells were then plated on Nutrient Agar plated with ampicillin. Colonies obtained were screened for PA-GFP and PA-mCherry by colony PCR using Taq. Polymerase using pCAG_F forward primer and PA-GFP/PAmCherry_Not1 reverse primer. Colonies showing bands around 1kb were selected and streaked on fresh nutrient agar plates with ampicillin and subsequently sent for sequencing with pCAF_F primer. Sequence results confirmed that PA-GFP and PA-mCherry were incorporated into the pCAG vector at the right position and orientation. The constructs were then digested with Age1 for 4 hours. To confirm the digestion had worked, the digested product was run on an 2% agarose gel. A band was observed at around 5.5kb as expected. The digested product was then treated with alkaline phosphatase (CIP) to prevent relegation of cut vectors. The Age1 digested lifeact PCR purified product was then ligated with the digested pCAG-PA-GFP / PA-mCherry, transformed into DH5α competent cells and plated on nutrient agar plates with ampicillin. The next day, PCR product of the colony PCR, using pCAG_F forward primer and lifeact_Age1 reverse primer, showed a band between 50 and 100bp on a 0.8% Agarose gel. The pCAG-lifeact –PA GFP / PA mCherry constructs were confirmed by sequencing with the same pCAG_F primer.

Non Neuronal Cell Culture

NIH3T3 cells were cultured in DMEM with 10% fetal bovine serum and penicillin / streptomycin and were maintained at 37°C. The cells were regularly passaged to maintain cultures.

Transfections of Non neuronal cells

At about 50 – 60 % confluency, 3T3 cells were transfected with lifeact constructs using a lipid based tranfection (Lipofectamine) method. The transfections were carried out in four well LABTEK culture chambers The cells were incubated in 400μL of OPTI-MEM for 20 min at 37°C. Meanwhile, a solution containing 3μL of lipofectamine, 1μg of plasmid (lifeact PAGFP / lifeact PAmCherry) was made upto 100μL with OPTI-MEM and incubated at room temperature for 20 min. This solution was then added to the cells and incubated at 37°C for 4 hours. The media was subsequently reverted to DMEM and incubated for at least 24 hours before imaging

Primary neuronal cultures

Embryonic days 8 dorsal root ganglion were removed from chick embryos and cut into smaller pieces in phosphate buffered solution (PBS). These explants were then cultured on acid washed coverslips coated first with 1mg/ml Poly-L-lysine for 6 hours and then with 20ug/ml laminin for 2 hours. The coverslips were mounted on holes drilled into the bottom of 35 mm Laxbro culture dishes. L-15 with B-27 additives and penicillin / streptomycin was used as culturing medium. The cultures were incubated overnight (18 hours) before experiment.

Preparation of NGF coated beads

Proteins (NGF and BSA) were covalently coupled to 10 μm diameter polystyrene carboxylated beads using the carbodiimide method. The protein coupling was performed as per the instruction provided by Poly-sciences. Carboxylated beads (2.5%w/v; 250 μl; containing about 1.137 X 10^7 beads) were washed twice with PolyLink Coupling Buffer (50mM MES, pH 5.2; 0.05% Proclin® 300). Washing involved centrifugation for 5-10 min at approximately 1000 X G in a microcentrifuge followed by aspiration of the supernatant and resuspension of bead pellet. After the washes the pellet was resuspended in 90 ul of PolyLink Coupling Buffer. Freshly prepared 10μl of 2% EDAC solution was added to the above suspension. This activation step was carried out for 30min with constant shaking. The beads were pellets down and the supernatant removed. The pellet was resuspended in coupling buffer containing 100ng/ml NGF and allowed to mix overnight. The next day, beads were pelleted and supernatant was stored at 0°C for determination of the amount of bound protein. Beads were subsequently washed twice with PolyLink Wash/Storage buffer (10mM tris, pH8.0; 0.05% BSA; 0.05% Proclin® 300). Particles were finally dissolved iin storage buffer and stored at -20°C.

Admittedly, the orientations of NGF bound to the surface of the bead were unknown. The carbodiimide reaction used to couple proteins to the beads could, in theory, link the L-, H- and A terminal groups with the activated C terminal group on the surface of the bead. Thus, NGF could have adopted several orientations on the bead surface.

Immunocytochemistry

Actin filaments were stained with Alexa 568 tagged to phalloidin. Indirect immunofluorescence of microtubules was carried out with polyclonal mouse primary anti-tubulin and secondary anti-mouse antibody conjugated with Alexa Flour 488 antibody. Cultures were fixed using 3.5% paraformaldehyde and 0.05% glutaraldehyde in warmed PHEM buffer for 10 min. Once rinsed, cultures were permeabilized with 0.1%

triton X in PHEM for 30 min after which they were blocked in 3% bovine serum albumin for about an hour. The cultures were then incubated in anti-tubulin antibody (1:3000) at 4°C overnight. The primary antibody was washed off and the cultures were once again blocked before incubation with secondary antibody and phalloidin for 2 hours at room temperature. The secondary antibody was then rinsed with PHEM.

Live imaging

Cultures were allowed to grow overnight before experimentation. For chronic treatment of cells with NGF, cultures were incubated with NGF at varied concentrations, overnight before imaging. Video microscopy was performed using differential interference contrast (DIC) on the Olymus IX81 inverted microscope. All observations were carried out at 37°C which was maintained with the help of OKO-lab bold line cage incubator (H201). Images were acquired at varied intervals depending on the experiment using the Hamamatsu CCD camera.

Analysis of Turning assay

Beads were added to cultured grown overnight and allowed to settle for 15 min. By visual inspection growth cone in the vicinity of beads were chosen and imaged by DIC. In experiment involving inhibitors, the drugs were added 30 min prior to start of the experiment. Observations continued till the growth cone either migrated under the bead or had advanced past the bead. To eliminate sampling bias, only growth cones that did not turn toward the bead after initial contact were chosen. Turning was defined by the movement of the growth cone's C- domain underneath the bead. Reorientation of the growth cone was defined as the displacement of the C-domain towards the bead but not underneath it, finally resulting in the C-domain being located past the bead. The main nerve fiber axis was defined as the line connecting the center of the C-domain with a point in the middle of the nerve fiber shaft 10μm behind the growth cones C domain, when the interaction had begun. The angle at which the growth cone migrated was then

determined by noting the center of the C-domain, 10 min after initial contact and drawing a line connecting this point with the point marking the center of the C-domain when the interaction had begun. The angle between the main nerve fiber axis, when the interaction had begun, and the line joining center of C-domain before and after translocation was defined as the turning angle.

Production of gradient by diffusion from coated micropipettes

Heat pulled capillaries tips were dipped in 2% nitrocellulose solution and dried. After drying, the tips were subsequently dipped in 5 μg/ml or BSA in PBS. The tips were then positioned 50 - 100μm from the growth cone at a 45° angle to the direction of direction of axon elongation, with the help of a manual micromanipulator. The positioning was performed in a closed OKO-LAB chamber maintained at 37°C. Images were then acquired at 30 sec interval for an hour (Ming et al., 1997).

Production of gradient by active ejection

5 – 20 ng/ml solution of NGF or BSA in PBS was continuously ejected through from a heat pulled capillary, with a diameter of less than 5μm, at a pressure of 5hPa. The capillary tip was placed at a 100μm from the growth cone. As the ejection was rapid and diffusion was slow, obtaining stable gradients was impossible. Hence the capillary tip was moved further away from the growth cone to allow for diffusion.

As the above two methods were done in a heated chamber, convectional flow hindered the formation of stable gradients.

CHAPTER 3

Results

3.1 Effects of actin nucleators on growth cone architecture and dynamics.

Actin nucleators are known to be involved in most processes which pertain to cytoskeletal dynamics. To test their involvement in growth cone dynamics, various techniques can be applied, like siRNA mediated knockdown, over expression studies, knockout studies, drug based inhibition. In this study, the role of Arp2/3 was identified by a inhibitory drug based approach. To quantify the effects on the growth cone, growth cone velocity, filopodia numbers, filopodia lengths and growth cone area were the parameters selected for comparison as actin nucleators are known to be involved in the formation of filopodia and lamellipodia, which indeed would affect translocation rates.

3.1.1 Arp2/3 in growth cone architecture and translocation

CK666 is a potent inhibitor of Arp2/3 complex. It prevents the complex from becoming active (Nolen et al., 2009).The DRG cultures were treated with 25μM CK666. This concentration was selected on the basis of earlier studies with this drug on *Aplysia* neurons, by Yang et. al. 2012, which showed that treatment with this inhibitor caused the dispersion of Arp2/3 complex from the C-domain, where it has been shown to be present (Yang et al., 2012).

To study the effects of Arp2/3 in the architecture and dynamics of growth cone, overnight cultured DRGs were treated with 25μM CK666 for 30 min, then fixed and stained with phalloidin to visualize actin. Finger like projections, stained with phalloidin, from the lamellipodia were counted and measured in length from the leading edge of the growth cone. There were no significant (Mann Whitney U test) differences in the filopodia numbers and lengths between the untreated (n=14) and DMSO treated controls (n=17) and also between the DMSO treated and CK666 treated growth cones

(n=15) (Figure 4A, B, & C). To look at the changes in the growth cone area and translocation rates, the growth cones were treated with 25μM CK666 (n=19) and DMSO (control, n=14) and imaged live. The growth cone areas were measured every 5min for 30min. An initial measurement was taken 5min prior to addition of the drug. The leading edge was traced through DIC, as shown in the Figure 4D and 4E, excluding the filopodia. To account for the intrinsic variation in the growth cone area, growth cone area was normalized with respect to time point just before the addition of the drug, CK666 or DMSO. The DMSO controls did not show any decrease in growth cone area. However, inhibition of Arp2/3, with CK666, decreased the area of the growth cone significantly (Figure 4F).

To calculate the translocation rates, average growth cone velocity (μm/min) was plotted for every 5 min after the addition of the CK666. However, like the DMSO controls, the translocation rates remained unaltered upon inhibition of Arp2/3 with CK666 (Figure 4G).

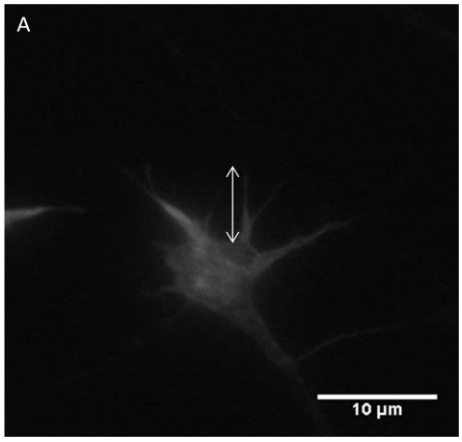

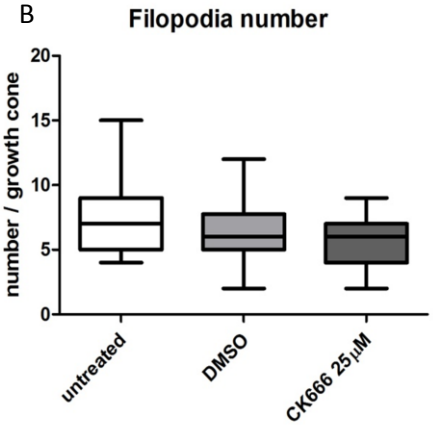

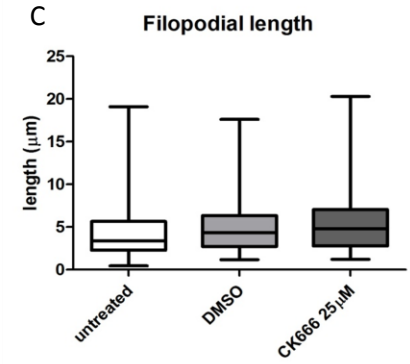

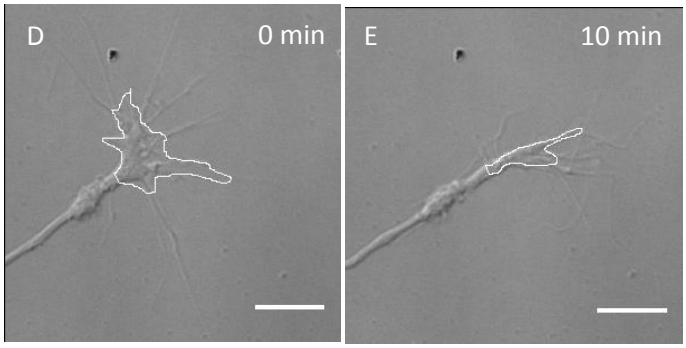

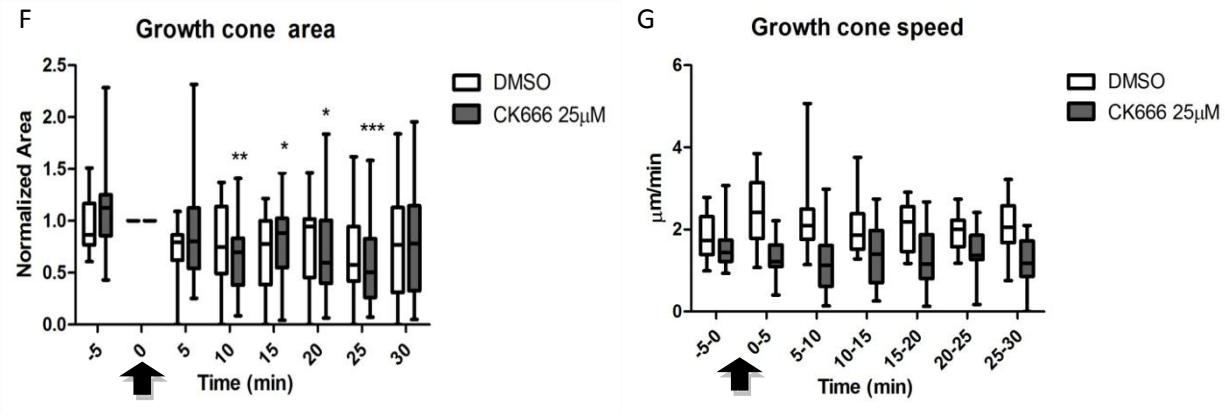

Figure 4: Arp2/3 inhibition affects the growth cone area but not speed or filopodia.(A) Representative figure showing how filopodia lengths were calculated. Double arrow head indicates the length of a filopodia. (B) shows the filopodia number per growth cone. (C) Filopodial length. (D-E) Representative figure, showing change in growth cone area. Growth cone area was measured 5min (-5) prior to addition of CK666 and then measured every 5min after addition. (F) Quantification of growth cone area. Arrow indicated addition of drug. (G) Translocation rates were measured every 5min from 5 min (-5) prior to addition of CK666. Arrow indicates the time point at which CK666 was added. Asterisks represent significance by Mann Whitney test. * - $p<0.05$; ** - $p<0.01$; *** - $p<0.001$

3.1.2 Inhibition of formins induce growth cone retraction

A generic inhibitor, small molecule inhibitor of FH2 (SMIFH2), of the FH2 domain containing proteins was used to impede the function of formins. In the initial experiments, higher concentrations of SMIFH2 (5μM) were used. This led to retraction nearly all the growth cones, almost instantly after addition of SMIFH2 (Figure 5B,C), though this concentration had been previously used on fibroblasts (Iskratsch et al.,

2013; Rizvi et al., 2009). The reduced concentration of SMIFH2 (1μM) induced retraction in nearly 70% of the growth cones within 5min after addition of the drug, which was significantly higher than the control (Figure 5A). Different formins are known to be involved in promoting cell adhesivity and generating traction forces and hence, it is possible that inhibition of all formins by SMIFH2 could lead to a loss in adhesion and traction, leading to retraction. Due to this retraction phenotype, which took place almost immediately after addition of SMIFH2, its architecture and translocation rates could not be determined.

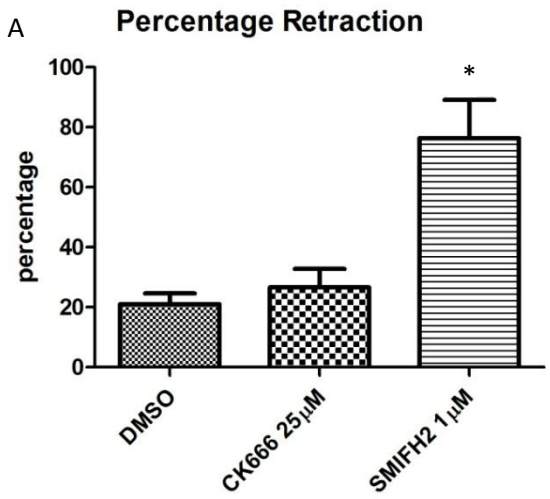

Figure 5: SMIFH2 treatment leads to growth cone retraction.
(A) Percentage retraction upon SMIFH2 treatment. Columns with error bars represent Mean with SEM. t-test * - $p<0.05$. (B-C) Representative pictures for retraction upon SMIFH2 treatment

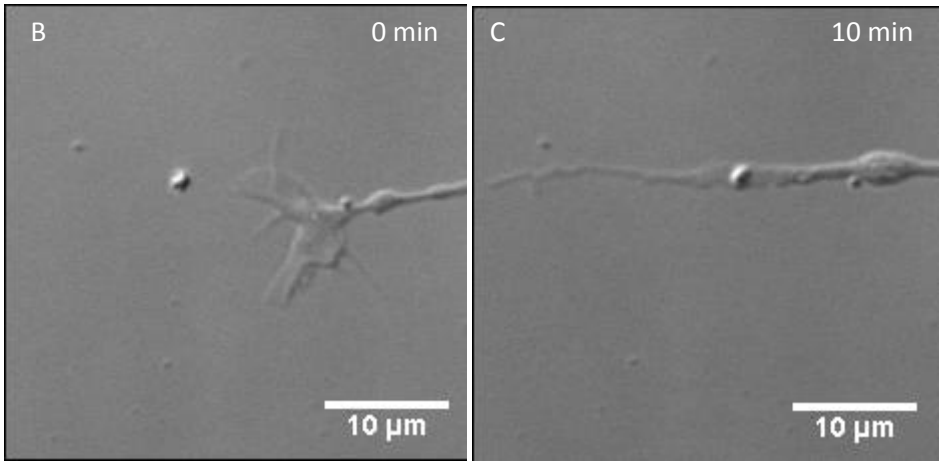

3.1.3 Inhibition of FH2 domain based actin nucleators in the background of Nerve Growth Factor

Since, addition of SMIFH2 led to retraction almost immediately after drug addition, cultures were treated with NGF to reduce retraction as NGF is known to promote and stabilize neuronal outgrowth. Thus, cultures were incubated with 20ng/ml of NGF overnight prior to SMIFH2 treatment. Qualitatively, the NGF addition reduced the retraction induced by SMIFH2. The growth cone architecture and dynamics were calculated similarly to growth cones with CK666 treatment.

The filopodial numbers decreased significantly with respect to the DMSO treated controls (Figure 6A). On the contrary, the filopodial lengths were unaffected with the addition of SMIFH2 (Figure 6B). Effect of inhibition of formins was tested by addition of 1 μM SMIFH2 to cultures grown overnight in media containing 20ng/ml NGF overnight. Also, treatment with SMIFH2 led to significant decrease in growth cone area when compared to DMSO controls (Figure 6C).

To assess the role of formins in growth cone dynamics, translocation rates were measured and compared, every 5min after treatment, for growth cones treated with 1μM SMIFH2 and DMSO. The SMIFH2 treated growth cones showed a significant decrease in the velocity while the DMSO controls remained unaltered (Figure 6D).

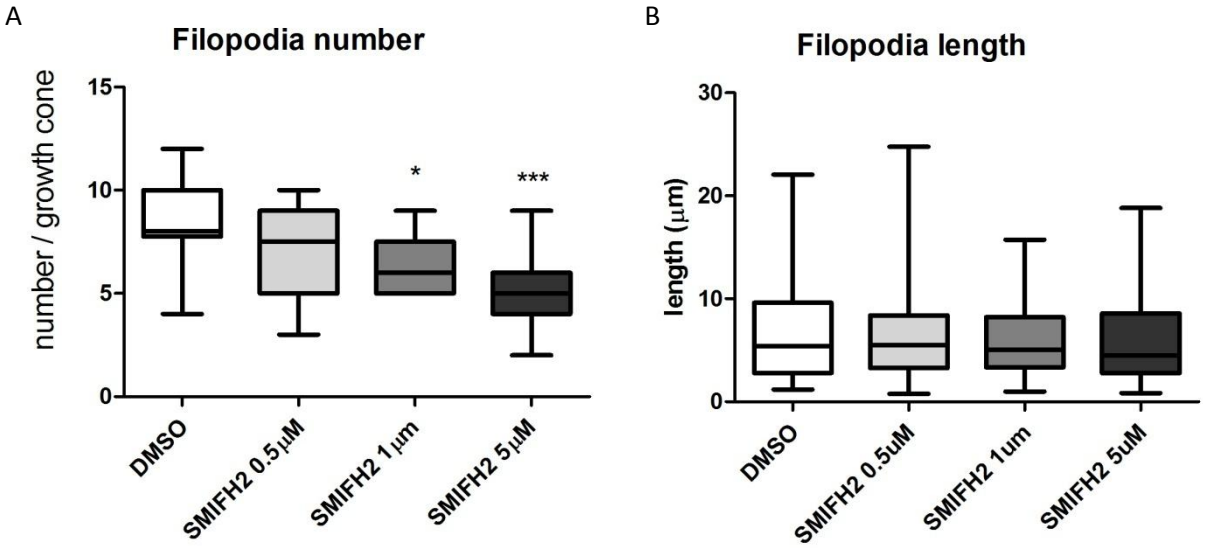

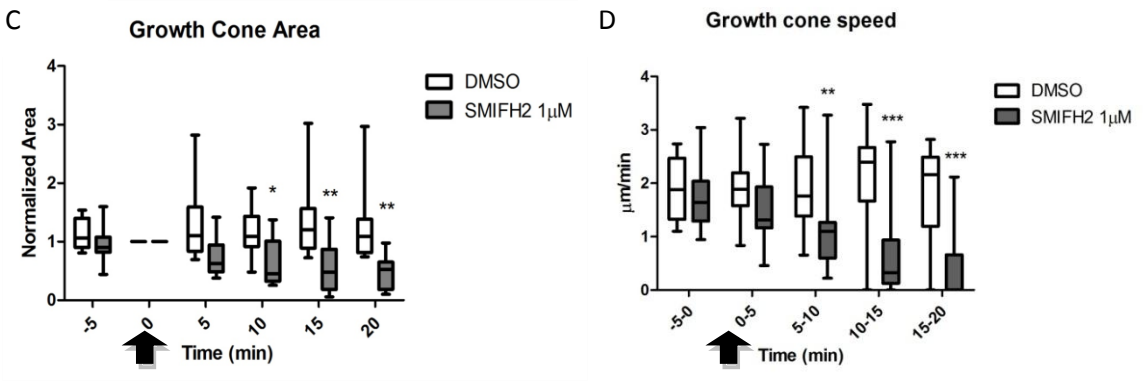

Figure 6: Effect of SMIFH2 on growth cones in the background of NGF. (A) Shows the filopodia number per growth cone. (B) Filopodial length. (C) Growth cone area was measured every 5min. Arrow indicates the time point at which SMIFH2 was added. (D) Translocation rates were measured every 5min. Columns with error bars represent Mean with SEM. Scale bar- 10μm . Arrow indicates the time point at which SMIFH2 was added. Asterisks represent significance by Mann Whitney U test. * - $p<0.05$; ** - $p<0.01$; *** - $p<0.001$

3.2 Turning assay

In order to test whether actin nucleators are involved in chemotropic directional movement of growth cones, pipette and bead based turning assays were developed.

3.2.1 Gradient generation by active ejection and diffusion from coated micropipettes

Initial rounds attempted involved active ejection of NGF from a small opening so as to create a gradient. NGF solution was expelled through pulled capillary of a diameter about 5 microns. The capillary tip was placed 100μm away from the growth cone at angle of 45° with respect to the direction of neurite extension. Continuous ejection of varied NGF concentrations at 5hPa was tested on advancing growth cones. The direction and length of extension were measured for 1 hour after the onset of the gradient. No discernible results were obtained in my hands using this protocol adapted from Poo et al. 1997. To assess if the gradients were being established in the first place, labeled BSA was added to the NGF solution. The diffusion of labeled BSA was minimal over 100μm as the ejection propelled the solution as a stream over this

distance. An easy solution to would be to place the capillary tip further away from the growth cone to allow for diffusion. But even this did not seem to solve the problem in generating stable gradients (Figure 7A-D).

An alternate approach, involving diffusion from a localized source coated with NGF, was pursued. This protocol was adapted from earlier work by Letourneau's group (Roche et al., 2009). In this assay, micropipette tips were coated with NGF. The tips were then placed near the growth cone at a distance of 50 to 100μm (Figure 7C,D). Convectional flow interfered with generation of stable gradients, resulting in inconclusive data.

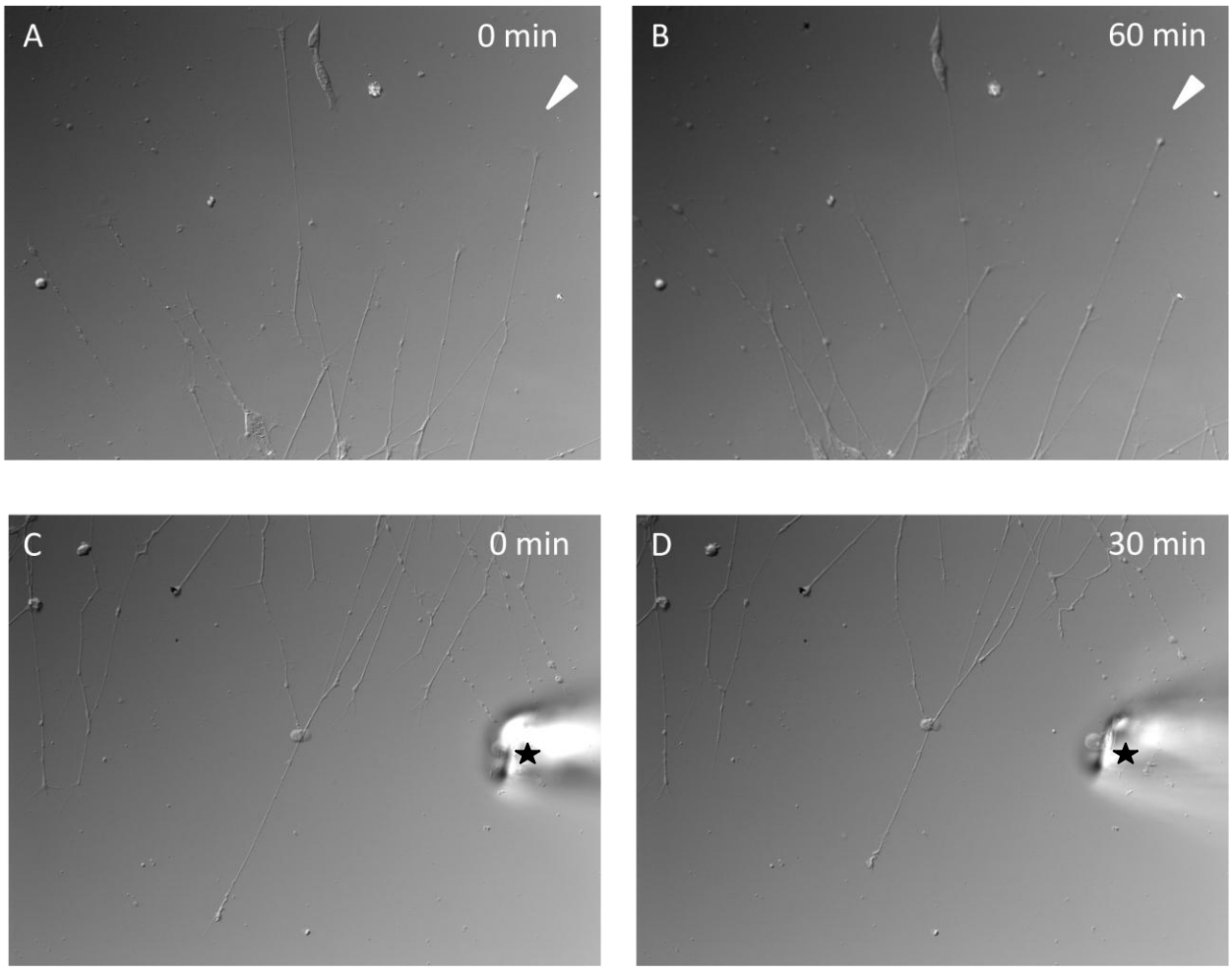

Figure 7: Diffusion based turning assay. (A-B) NGF was continuously ejected in the direction of the arrow head for 1 hour. (C-D) NGF coated micropipettes (star) were used to generate gradients. This usually resulted in resulted in the retraction of nearby growth cones.

3.2.2 Development of a NGF coated bead based turning assay

NGF and BSA coated bead were added to DRG cultures grown overnight. Once the beads had settled and growth cones had contacted the bead, imaging commenced at regular intervals of 30 sec. Response of the growth cone was characterized in to three classes;

1. Turn – When growth cone turned towards the contacted bead (Figure 8A-D).
2. Pull – Sometimes, the contacted beads were pulled on to the central domain of the growth cone (Figure 8E-H).
3. Ignore – This category includes all growth cones that contacted a bead but did not show any response, rather continued advancing without turning or pulling the bead (Figure 8I-L).

Almost 50% percent of the DRG growth cones that contacted the NGF coated bead (n=19) turned towards it, while only about 30% of the growth cones showed a turning response towards a BSA coated beads (n=15). Instances where the growth cone pulled the bead were higher in case of the NGF coated beads (~30%) when compared to that of BSA coated beads (~16%). Pulling can be an inferred as an extreme form of attraction, where the growth cone is able to dislodge the bead from its initial position and pull it onto itself. On the other hand, a higher percentage of growth cones seemed to ignore the BSA coated beads (>50%) where as a mere 20% ignored the NGF coated beads (Figure 8M).

The turning response showed certain characteristic behaviours. First, it was initiated by a filopodium contacting the bead, followed by either strengthening of the filopodial contact by thickening along the filopodia. Sometimes the growth cones side stepped (lateral movement) towards the bead. As the contact strengthened, it underwent engorgement i.e. cytoplasm moved towards the contact. Finally, growth appeared to be moving from underneath the bead and protruding growth cone structures from the distal end.

The response of the growth cone was almost immediate after contact. Within 10 minutes of initial contact, more than 90% of the growth cones had elicited a response. This is in accord with earlier report, which suggested that the mean time for turning is about 9 minutes (Gallo et al., 1997). These results suggest that growth cones preferentially turn with a higher probability towards NGF coated beads and that growth cones, although with low probability, can intrinsically turn towards any object that they encounter.

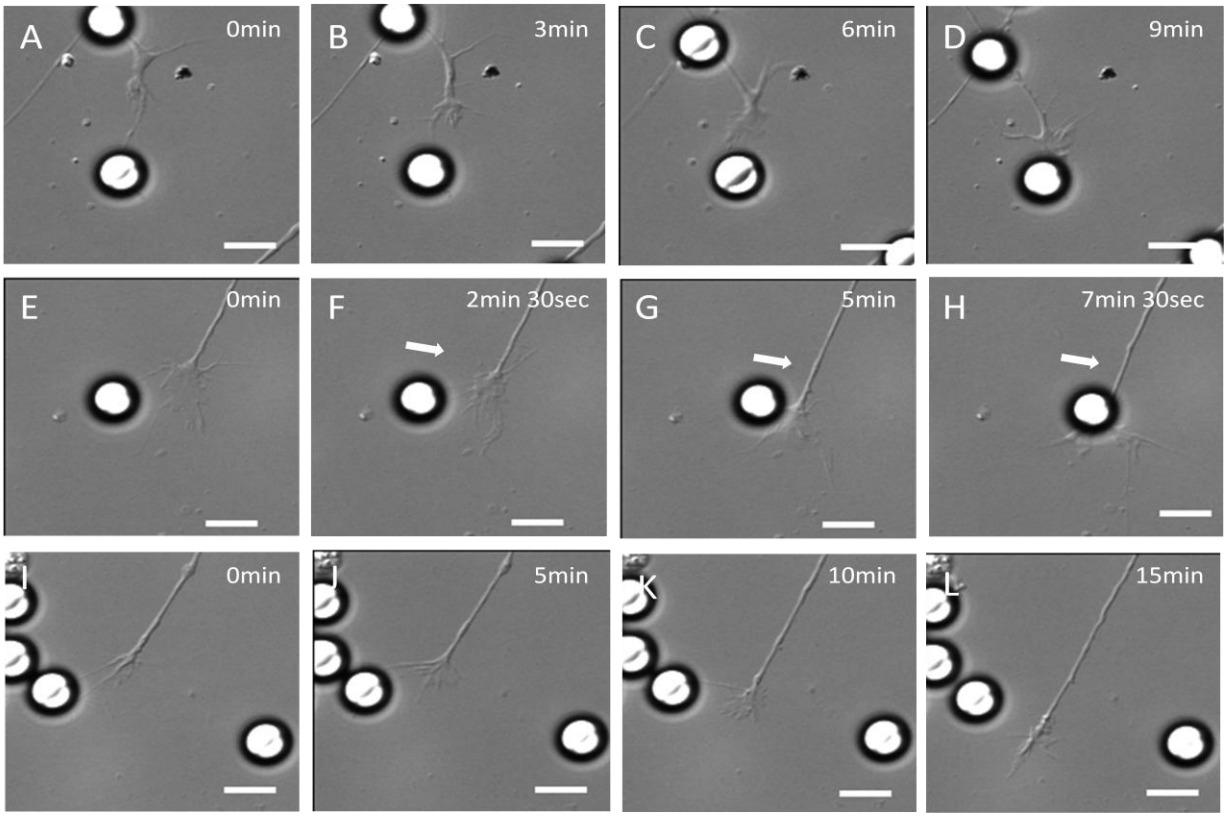

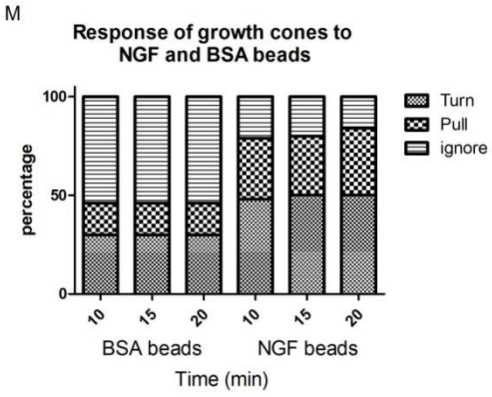

Figure 8: Growth cone response to NGF and BSA coated beads. (A-D) Example of growth cone turning towards NGF coated bead. Initial filopodial contact was established at 0 min. this was followed by thickening along the contact (3min). By 6 min, cytoplasmic engorgement took place and by the end of 9 min, the growth cone was under the bead. Scale bar: 5μm. (E-H) Example of a NGF coated bead being

picked up by a growth cone. The arrow indicates the direction in which the bead was displaced. Scale bar : 5μm. (I-L) Example of growth cone ignoring the BSA coated bead. Initial contact was established, which persisted over 10 min but even then the growth did not turn towards the bead. Scale bar : 5μm. (M) Percentage plot showing the behavior of growth cones coming in contact with BSA (n=15) or NGF (n=19) coated beads, with respect to time. Most of the growth cones had elicited a response within 10 min.

3.2.3 Arp2/3 is involved in growth cone turning

To test the involvement of Arp2/3 and formins on growth cone behavior upon contacting a NGF bead, the cultures were incubated with the drug 30 min prior to the start of the turning assay. Figure 9A shows the comparison between CK666 treated and untreated growth cones. From the graph it is clear that DRG growth cones show loss in ability to turn towards NGF coated beads once Arp2/3 is inhibited. In fact, a higher percentage (~70%) of growth cones ignore the NGF coated bead compared to untreated growth cones ignoring BSA coated beads. Figure 9B shows the cumulative distribution of growth cones and there response to NGF beads. Similar experiments were performed by inhibiting formins, using the SMIFH2 drug. But retraction and the inability of growth cones to advance precluded SMIFH2 analysis with bead based turning assay.

Turning angles were plotted 10 min after initial contact (Figure 9B). The side of the contact was considered as positive and the other side as negative.

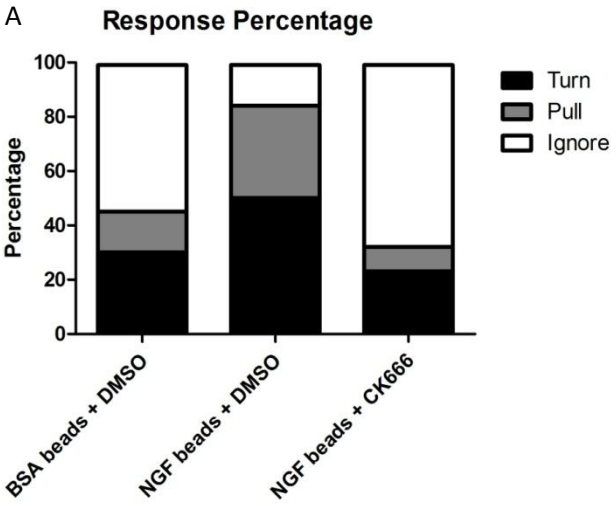

Figure 9: Arp2/3 is involved in turning. (A) Percentage plot comparing response between CK666 and controls. (B) Cumulative distribution of turning angles. Green curve – growth cones response to NGF coated beads; Blue curve – growth cone response to BSA coated beads; Red curve – response of growth cones bath treated with CK666, to NGF coated beads

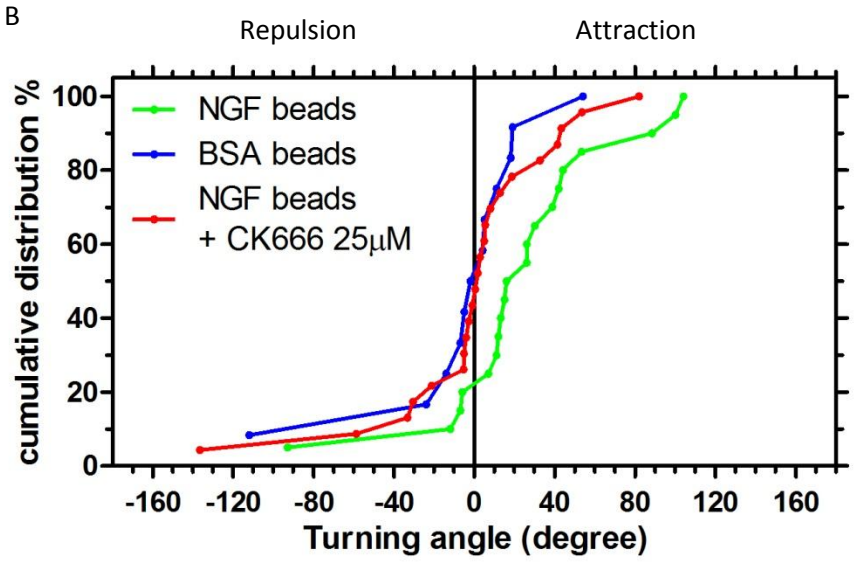

3.3 Effects of acute NGF treatment on Growth cones

Chemo-attractant and chemotropic agents may induce extension of protrusions like filopodia and lamellipodia. In order to test the role of actin nucleators in generating induced protrusion, I developed the assay based on acute bath treatment with NGF. The effects of nerve growth factor (NGF) on growth cones was assessed by application of NGF to cultured embryonic day 8 chick dorsal root ganglion (DRG) which have been overnight without NGF. Upon application of 50ng/ml NGF, the growth cones of these DRGs were imaged at 30sec interval for 30min. Only two factors could be taken into

consideration: growth cone area and velocity, as the the NGF induction led to massive enhancement of lamellipodial protrusion which dominated over the filopodia. Both factors, the translocation rate and growth cone area, showed a significant difference when compared to control (vehicle). The increase in growth cone area was almost two fold higher within 10 minutes after the induction of NGF (Figure 10A-D,I). No significant difference was noticed in the control (Figure 10E-H,I).

The growth cone speed reduced in the NGF treated DRGs compared to that of the control (Figure 10J). The controls on the other hand maintained almost the same velocity upon vehicle induction.

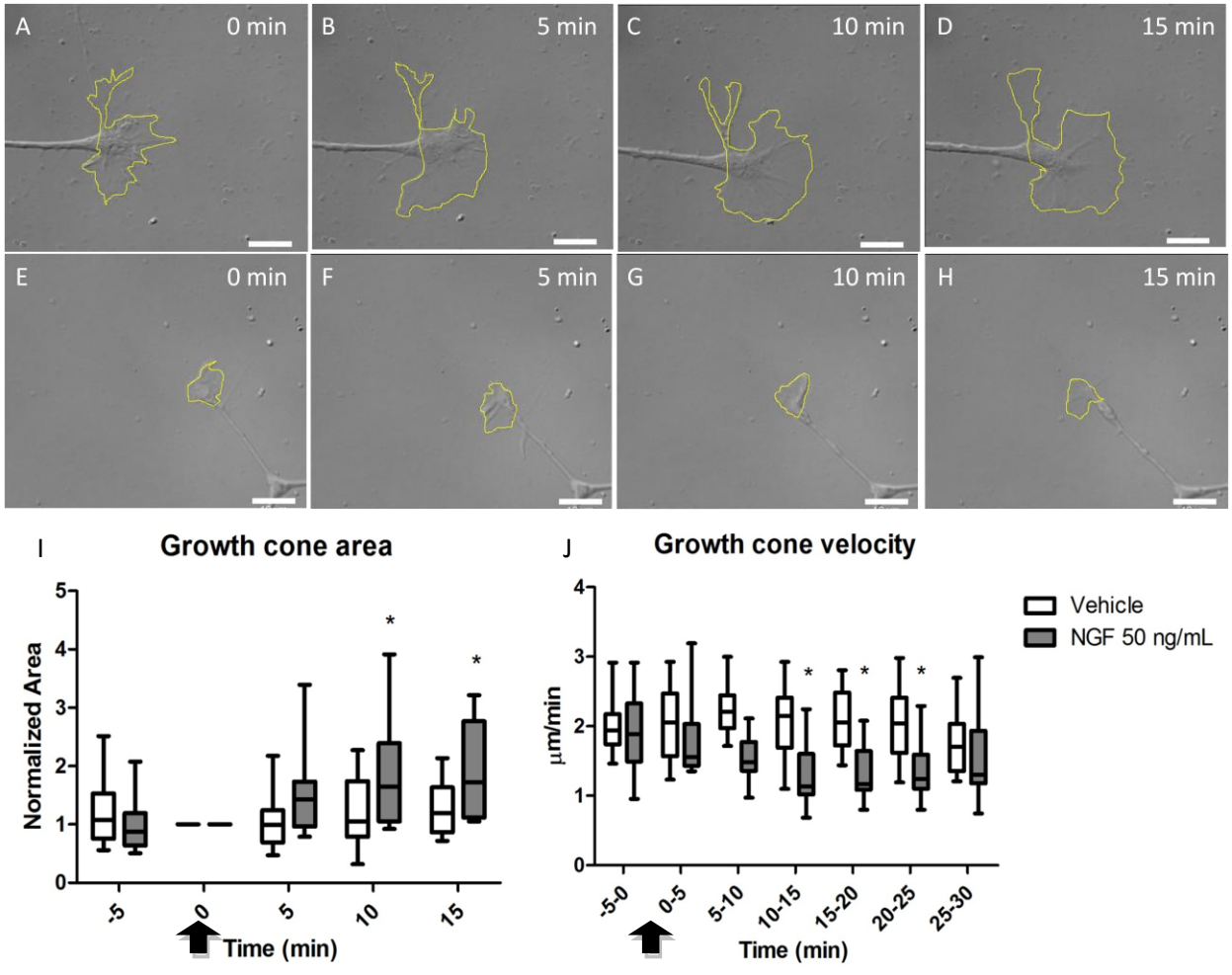

Figure 10: Effect on growth cone upon induction of NGF. (A-D) DRGs treated with 50ng/ml NGF overnight. Growth cone area is outlined in yellow. Scale bar – 10µm. (E-H) DRGs treated with control vehicle. Area outlined in yellow. Scale bar – 10µm. (I)

Quantification of growth cone area. Area was normalized to 0sec time point i.e. just before induction of vehicle or NGF. (J) Quantification of growth cone speed. Arrow indicates the time point at which NGF or vehicle was added. Mann Whitney U test. * - $p<0.05$; ** - $p<0.01$; *** - $p<0.001$

3.4 Development of reagents for super-resolution imaging of actin structures

Some formins have been shown to localize on stress fibers and our results showed that inhibition of formins by SMIFH2 led to decrease in translocation rates and also retraction. Therefore, it is reasonable to say that formins are needed for cell adhesion and generations of traction forces. As stress fibers play a role in maturation of focal adhesions, looking at the effects of formins on stress fibers could provide some insight on how formins influence the cell adhesivity. To quantify the effects on stress fibers, it would be judicious to develop tools to visualize actin stress fibers. By developing tools for super-resolution imaging, we can accurately note the changes on stress fibers by individually knocking down formins.

Photo-activatable GFP (PA-GFP) and photo-activatable mCherry (PA-mCherry) were cloned to the N terminus of lifeact and incorporated into a chick neuron and mammalian expressing vector (pCAG) (See Materials and Methods). Cloning photo-activatable constructs with lifeact would help us deduce actin dynamics by PALM (photoactivated localization microscopy) super resolution microscopy.

Both these photo-activatable constructs were tranfected into 3T3 cell lines and incubated overnight. The next day, the transfected cells were activated by 405 nm laser. Following activation, these photo-activatable constructs were excited with 488 nm, for PAGFP, and 561 nm, for PAmCherry. Figure 11(A-D) shows that after activation, lifeact is detected in the cytosol and also decorates the actin stress fibers. lifeact-PAGFP and lifeact-PAmCherry were activated by 405 nm illumination in widefield mode without a defined ROI. Figure 11(E-H,I) shows the activation of lifeact-PAmCherry by a laser scanning confocal microscope with a defined rectangular ROI. Preliminary results suggest that these constructs are working and could used to develop super resolution tools.

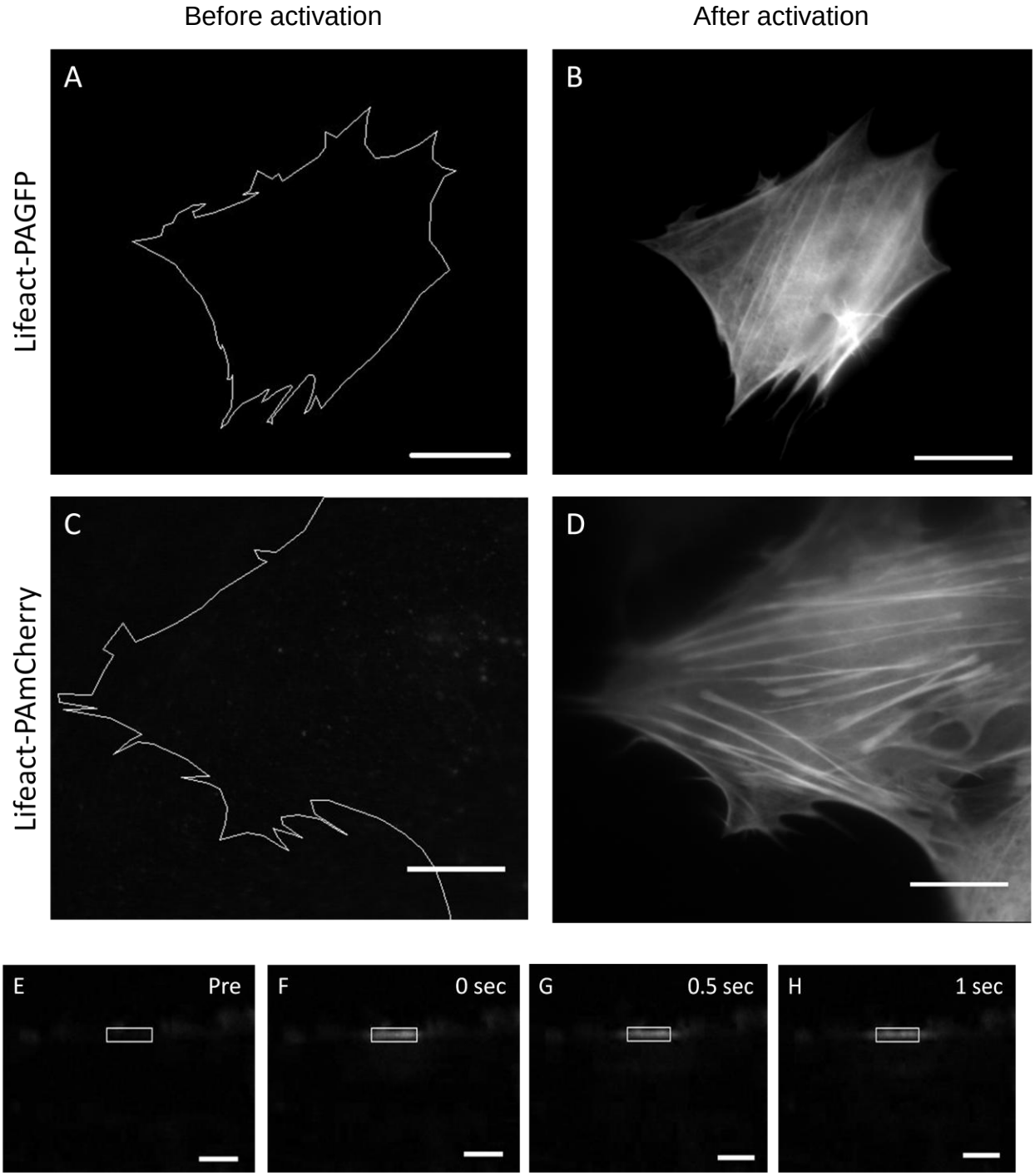
Before activation
After activation
Lifeact-PAGFP
Lifeact-PAmCherry
A
B
C
D
E
Pre
F
0 sec
G
0.5 sec
H
1 sec

I

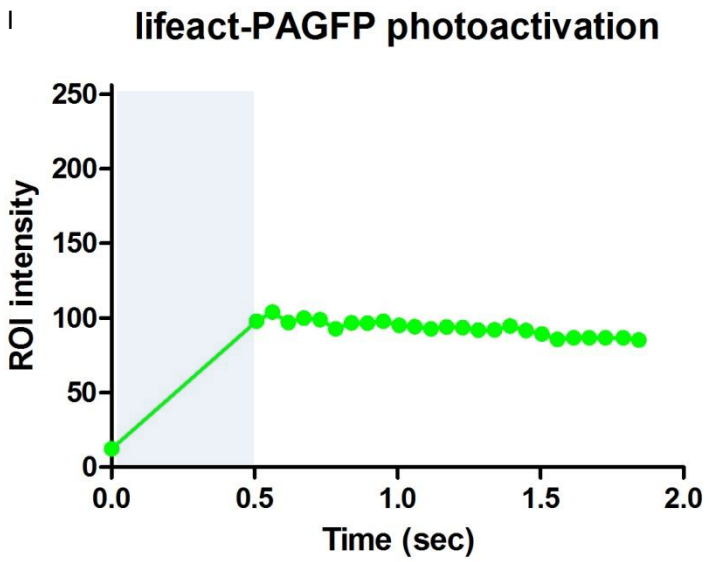

Figure 11: Activation of lifeact photoactivatable constructs. (A-D) shows the activation of lifeact PA-GFP and lifeact PA-mCherry. Activation was carried out for 2 sec with 405 nm laser at 100% intensity without defined ROI. Scale bar- 10µm. (E-H) shows the activation of lifeact PA-mCherry. Scale bar- 10µm. (I) ROI intensity plot of lifeact PA-mCherry upon photo-activation. Blue region in the graph represents photo-activation.

3.5 Developing FRAP analysis for stress fiber dynamics

Another important factor to look at is the stress fiber dynamics after knocking down formins. Modeling the recovery rates after photobleaching actin-GFP on stress fibers, could answer some questions as to how stress fiber dynamics are affected by formins. Unpublished data from our lab shows that formins, especially formin2, localize on stress fibers and their depletion results in compromised stress fiber structures. This suggests the involvement of formins in the formation and maintenance of stress fibers (Abhishek Sahasrabudhe).

In preliminary experiments, NIH3T3 cells were transfected with actin-GFP to perform FRAP analysis in order to obtain actin dynamics at stress fibres. The photo-bleaching was performed at various locations on the stress fibers - at the site of focal adhesion,

near focal adhesions and far from the focal adhesions. Fluorescence recovery was observed at these locations and plotted (Figure 12A, B). In these preliminary, proof of principle experiments (n=2), qualitative assessment of data suggests that the bleached region at the FA recovers faster than those away from it. The preliminary data indicates is that this strategy is likely to work and in combination with siRNA mediated depletion of specific molecules may uncover regulatory functions at the stress fibres.

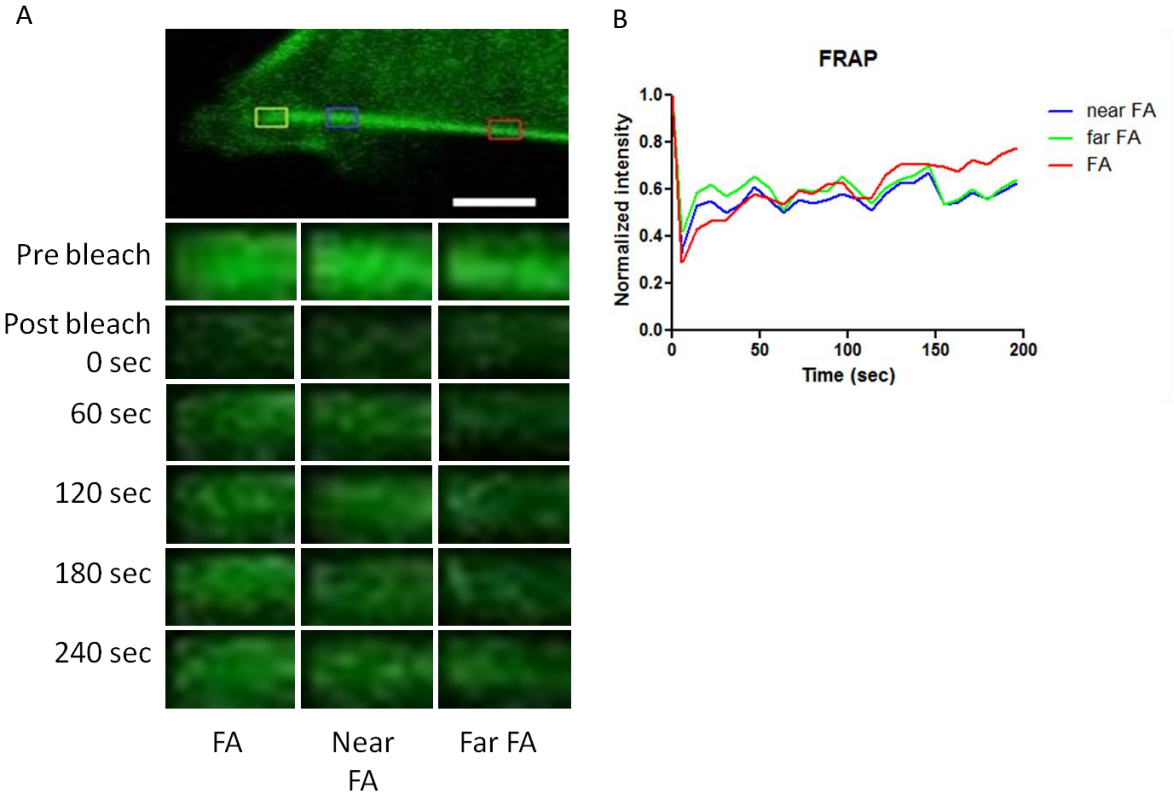

Figure 12: Fluorescence recovery after photobleaching of actin-GFP. (A) FRAP performed on selected ROIs. Green ROI- Focal Adhesion, Blue ROI – near FA, Red ROI- far FA. Inset show the various ROIs. Scale bar- 5µm. (B) Quantification of Fluorescence recovery after bleaching.

CHAPTER 4

Discussion

4.1 Role of Arp2/3 in growth cone architecture and dynamics

Arp2/3 forms branched actin filaments which generate protrusive force to extend lamellipodia. In growth cones, Arp2/3 is enriched in the C domain and also the leading edge of the P domain. Thus, it is expected that Arp2/3 also plays similar roles here. Earlier studies involving knockdown and inhibition of Arp2/3 have given conflicting results. Using siRNA knockdown it was shown, that depletion of Arp2/3 led to retardation of translocation rates (Korobova and Svitkina, 2008) but functional inhibition of this protein complex leads to increase in the axon elongation (Strasser et al., 2004). Use of CK666 in *aplysia* growth cones has shown that, inhibition of Arp2/3 leads to decrease in the veil like actin structure which comprises the lamellipodia decreases without affecting the filopodia number and length (Yang et al., 2012). Our results with inhibition of Arp2/3 with CK666, are similar to the earlier studies in *Aplysia* with CK666. In this study, we show that Arp2/3 does not affect filopodia, nor does it affect the translocation rates. But inhibition does lead to a significant decrease in the growth cone area. This is in congruence with the model that Arp2/3 is involved in lamellipodial formation. Looking at kymographs of the Arp2/3 growth cone treated growth cones, would give us a better understanding the Arp2/3 complex in generating protrusions.

4.2 Role of formins in growth cone architecture and dynamics

Formins contains a huge class of proteins which have a broad range of functions. Our lab has shown that formin2 knockdown by morpholinos induces reduction in filopodial lengths but not numbers (unpublished; Abhishek Sahasrabudhe). Other groups have shown that mDia is involved in growth cone retraction mediated (Toyoda et al., 2013). formins have been shown to localize on stress fibers and also mediate its formation (Lammel et al., 2014; Takeya et al., 2008). Apart from stress fibers, mDia group of formins is also known to regulate focal adhesion dynamics (Gupton et al., 2007). Thus, these nucleators are involved in generating traction forces to generate motility. Inhibition of these ormins could lead to loss in adhesion between the growth cone and the substrate, prompting retraction. My results show that inhibition of formins by SMIFH2 leads to retraction which is in agreement with various roles that formins have. Although a small population of growth remained upon treatment, this could represent a different population of neurons which are slightly resistant to SMIFH2. To better understand the effects of formins, cultures grown overnight with NGF, which promotes growth and health of neurons, were treated with SMIFH2. Results from these experiments suggest that formins could be involved in the formation and maintenance of filopodia. Also, formins are mediate growth cone motility.

4.3 Arp2/3 mediates growth cone turning

This was the first time a localized source based turning assay was attempted to check whether actin nucleators are involved in turning. A preferential turning toward NGF coated beads was observed in comparison to BSA coated beads. The turning response was fast and reached completion within 10 minutes following first contact with the bead. In some instances, the growth cone oriented and attached itself to the bead so strongly that it displaced the bead towards it. Thus pulling can be considered an extreme case of attraction. Pretreatment with CK666, led to loss in the attraction of growth cones towards NGF beads. This suggested that Arp2/3 is indeed involved in a turning response. Localization/activation of Arp2/3 towards the side of attractant could lead to

directional movement of the growth cone towards the bead. No results could be obtained with respect to SMIFH2 treated growth cones as it prevented growth cones from advancing and in most cases retraction.

In the future, this assay will be used to look at individual formins and their role in turning.

4.4 Effect of acute NGF treatment

NGF induction led to increased lamellipodial protusivity, increasing the growth cone area almost two fold. This lamellipodial protrusion could arise due to NGF induced stabilization of the underlying actin meshwork. NGF acts as a chemo-attractant and can activate various downstream elements that remodel the cytoskeleton. Comparison of motility and growth cone morphology, between NGF treated and untreated, shows that though NGF treated growth cones increase in area, though average speed seems to reduce. Thus, the growth cones seem adhere more strongly upon induction of NGF. Without NGF, complete blockage of formins leads to retraction. This assay could be used to study the role of formins by individual formin knockdown.

4.5 Super resolution and FRAP to study actin stress fiber dynamics

Actin dynamics in stress fibers play an important role in movement of a cell. To study these dynamics, it is necessary to develop the necessary tools. By cloning lifeact with photoactivatable proteins, one can visualize actin dynamics on a faster time scale, as lifeact is known to have a short turnover period. By stochastically activating a small group of these tagged proteins one can construct a super resolved image.

From the qualitative analysis of the preliminary FRAP experiments, it appears that the recovery at the focal adhesion is fastest. Also, the bleached areas away from the focal adhesion on the stress fiber recover slowly. Though only preliminary, it agrees with the model that more barbed ends are available for binding near the FA compared to a

region distant on the stress fibers. In the future, this tool can be used to look at the role of formins in stress fiber dynamics by siRNA mediated knockdown.

References:

Breitsprecher, D., and Goode, B.L. (2013). Formins at a glance. Journal of Cell Science *126*, 1–7.

Campellone, K.G., and Welch, M.D. (2010). A nucleator arms race: cellular control of actin assembly. Nature Reviews. Molecular Cell Biology *11*, 237–251.

Chesarone, M. a, DuPage, A.G., and Goode, B.L. (2010). Unleashing formins to remodel the actin and microtubule cytoskeletons. Nature Reviews. Molecular Cell Biology *11*, 62–74.

Dominguez, R. (2009). Actin filament nucleation and elongation factors--structure-function relationships. Critical Reviews in Biochemistry and Molecular Biology *44*, 351–366.

Firat-Karalar, E.N., and Welch, M.D. (2011). New mechanisms and functions of actin nucleation. Current Opinion in Cell Biology *23*, 4–13.

Gallo, G., Lefcort, F.B., and Letourneau, P.C. (1997). The trkA receptor mediates growth cone turning toward a localized source of nerve growth factor. The Journal of Neuroscience : the Official Journal of the Society for Neuroscience *17*, 5445–5454.

Gomez, T.M., and Letourneau, P.C. (2013). Actin dynamics in growth cone motility and navigation. Journal of Neurochemistry 1–14.

Gupton, S.L., Eisenmann, K., Alberts, A.S., and Waterman-Storer, C.M. (2007). mDia2 regulates actin and focal adhesion dynamics and organization in the lamella for efficient epithelial cell migration. Journal of Cell Science *120*, 3475–3487.

Henley, J.R., and Poo, M. (2011). Guiding Neuronal Growth Cones by Ca2+ Signals: During axon pathfinding in the developing nervous system, spatiotemporal patterns of Ca2+ signals can govern growth cone extension and steering—by symmetric versus asymmetric regulation of cytoskeletal and me. Trends in Cell Biology *14*, 320–330.

Iskratsch, T., Yu, C.-H., Mathur, A., Liu, S., Stévenin, V., Dwyer, J., Hone, J., Ehler, E., and Sheetz, M. (2013). FHOD1 is needed for directed forces and adhesion maturation during cell spreading and migration. Developmental Cell *27*, 545–559.

Jin, M., Guan, C., Jiang, Y., Chen, G., Zhao, C., Cui, K., Song, Y., Wu, C., Poo, M., and Yuan, X. (2005). Ca2+-dependent regulation of rho GTPases triggers turning of nerve growth cones. The Journal of Neuroscience : the Official Journal of the Society for Neuroscience *25*, 2338–2347.

Korobova, F., and Svitkina, T. (2008). Arp2 / 3 Complex Is Important for Filopodia Formation , Growth Cone Motility , and Neuritogenesis in Neuronal Cells. *19*, 1561–1574.

Kovar, D.R. (2006). Molecular details of formin-mediated actin assembly. Current Opinion in Cell Biology *18*, 11–17.

Kovar, D.R., Kuhn, J.R., Tichy, A.L., and Pollard, T.D. (2003). The fission yeast cytokinesis formin Cdc12p is a barbed end actin filament capping protein gated by profilin. The Journal of Cell Biology *161*, 875–887.

Lammel, U., Bechtold, M., Risse, B., Berh, D., Fleige, A., Bunse, I., Jiang, X., Klämbt, C., and Bogdan, S. (2014). The Drosophila FHOD1-like formin Knittrig acts through Rok to promote stress fiber formation and directed macrophage migration during the cellular immune response. Development (Cambridge, England) 1–15.

Lowery, L.A., and Van Vactor, D. (2009). The trip of the tip: understanding the growth cone machinery. Nature Reviews. Molecular Cell Biology *10*, 332–343.

Ming, G.L., Song, H.J., Berninger, B., Holt, C.E., Tessier-Lavigne, M., and Poo, M.M. (1997). cAMP-dependent growth cone guidance by netrin-1. Neuron *19*, 1225–1235.

Mullins, R.D., Heuser, J. a, and Pollard, T.D. (1998). The interaction of Arp2/3 complex with actin: nucleation, high affinity pointed end capping, and formation of branching networks of filaments. Proceedings of the National Academy of Sciences of the United States of America *95*, 6181–6186.

Nolen, B.J., Tomasevic, N., Russell, a, Pierce, D.W., Jia, Z., McCormick, C.D., Hartman, J., Sakowicz, R., and Pollard, T.D. (2009). Characterization of two classes of small molecule inhibitors of Arp2/3 complex. Nature *460*, 1031–1034.

Pollard, T.D., and Borisy, G.G. (2003). Cellular motility driven by assembly and disassembly of actin filaments. Cell *112*, 453–465.

Pollard, T.D., and Cooper, J. a (2009). Actin, a central player in cell shape and movement. Science (New York, N.Y.) *326*, 1208–1212.

Riedl, J. (2010). Development and Characterization of Lifeact - a versatile marker for the visualization of F-actin -.

Riedl, J., Crevenna, A.H., Kessenbrock, K., Yu, J.H., Neukirchen, D., Bradke, F., Jenne, D., Holak, T.A., Werb, Z., Sixt, M., et al. (2008). Lifeact : a versatile marker to visualize F-actin. *5*, 605–607.

Rizvi, S. a, Neidt, E.M., Cui, J., Feiger, Z., Skau, C.T., Gardel, M.L., Kozmin, S. a, and Kovar, D.R. (2009). Identification and characterization of a small molecule inhibitor of formin-mediated actin assembly. Chemistry & Biology *16*, 1158–1168.

Roche, F.K., Marsick, B.M., and Letourneau, P.C. (2009). Protein synthesis in distal axons is not required for growth cone responses to guidance cues. The Journal of Neuroscience : the Official Journal of the Society for Neuroscience *29*, 638–652.

Ruiz-Cañada, C., and Budnik, V. (2006). Synaptic cytoskeleton at the neuromuscular junction. International Review of Neurobiology *75*, 217–236.

Schönichen, A., and Geyer, M. (2010). Fifteen formins for an actin filament: a molecular view on the regulation of human formins. Biochimica Et Biophysica Acta *1803*, 152–163.

Sept, D., and McCammon, J. a (2001). Thermodynamics and kinetics of actin filament nucleation. Biophysical Journal *81*, 667–674.

Smertenko, a. P., Deeks, M.J., and Hussey, P.J. (2010). Strategies of actin reorganisation in plant cells. Journal of Cell Science *123*, 3029–3029.

Strasser, G.A., Rahim, N.A., Vanderwaal, K.E., Gertler, F.B., and Lanier, L.M. (2004). Arp2 / 3 Is a Negative Regulator of Growth Cone Translocation. Neuron *43*, 81–94.

Sun, S.-C., Wang, Z.-B., Xu, Y.-N., Lee, S.-E., Cui, X.-S., and Kim, N.-H. (2011). Arp2/3 complex regulates asymmetric division and cytokinesis in mouse oocytes. PloS One *6*, e18392.

Sun, S.-C., Wang, Q.-L., Gao, W.-W., Xu, Y.-N., Liu, H.-L., Cui, X.-S., and Kim, N.-H. (2013). Actin nucleator Arp2/3 complex is essential for mouse preimplantation embryo development. Reproduction, Fertility, and Development *25*, 617–623.

Takeya, R., Taniguchi, K., Narumiya, S., and Sumimoto, H. (2008). The mammalian formin FHOD1 is activated through phosphorylation by ROCK and mediates thrombin-induced stress fibre formation in endothelial cells. The EMBO Journal *27*, 618–628.

Toyoda, Y., Shinohara, R., Thumkeo, D., Kamijo, H., Nishimaru, H., Hioki, H., Kaneko, T., Ishizaki, T., Furuyashiki, T., and Narumiya, S. (2013). EphA4-dependent axon retraction and midline localization of Ephrin-B3 are disrupted in the spinal cord of mice

lacking mDia1 and mDia3 in combination. Genes to Cells : Devoted to Molecular & Cellular Mechanisms *18*, 873–885.

Yang, Q., Zhang, X.-F., Pollard, T.D., and Forscher, P. (2012). Arp2/3 complex-dependent actin networks constrain myosin II function in driving retrograde actin flow. The Journal of Cell Biology *197*, 939–956.

Zigmond, S.H. (2004). Formin-induced nucleation of actin filaments. Current Opinion in Cell Biology *16*, 99–105.